This is an extended version of the paper presented in SEE7 conference, peer-reviewed again and approved by the JSEE editorial board.

Numerical Evaluation of the Strike-Slip Fault Effects on the Steel Buried Pipelines

Hossein Tahghighi[1*] and M. Mehdi Hajnorouzi[2]

1. Assistant Professor, University of Kashan, Kashan, Iran,
* Corresponding Author; email: tahghighi@kashanu.ac.ir
2. M.Sc. Student, University of Kashan, Kashan, Iran

Received: 01/09/2015
Accepted: 16/12/2015

ABSTRACT

Pipelines are often referred to as lifelines, demonstrating that they play an important role in human's life. Based on the damage mechanism, the permanent ground movements of active faults can have the most severe earthquake effects on buried pipelines. In this study, the effects due to strike-slip faulting have been investigated using 3D FEM, Winkler model and analytical method. The non-linear response of buried pipeline under fault offset is analyzed using pseudo-static approach wherein the interacting soil-pipeline system is modeled rigorously. The paper focuses on the effects of soil and pipeline parameters on the structural response of the pipe, with particular emphasis on identifying pipeline failure. Some influential factors, such as fault-pipeline crossing angle, backfill type, burial depth, pipe diameter to thickness ratio and pipe surface characteristics are considered in the analyses in order to draw some regular conclusions. The present investigation is aimed at determining the fault displacement at which the pipelines fail for design purposes.

Keywords:
Buried pipeline; Fault movement; Strike-slip; Non-linear response

1. Introduction

Earthquakes may constitute a threat for the structural integrity of buried pipelines. Post-earthquake investigations have demonstrated that the majority of seismic damages to continuous oil and gas steel pipelines were caused by permanent ground deformations such as fault movements, landslides, liquefaction-induced lateral spread, whereas only few pipelines were damaged by wave propagation. Permanent fault displacement is applied on the pipeline in a quasi-static manner, and it is not necessarily associated with high seismic intensity, but the pipeline may be seriously damaged. Surface faulting has accounted for many pipe breaks during past earthquakes, such as the 1971 San Fernando (USA), the 1995 Kobe (Japan), the 1999 Izmit (Turkey), the 1999 Chi-Chi (Taiwan) events and more recently, the 2004 Mid Niigata earthquake in Japan [1-3]. Apart from the detrimental effects that such a rupture can have to the operation of critical lifeline systems, an irrecoverable ecological disaster may also result from the leakage of environmentally hazardous materials such as natural gas, fuel or liquid waste.

Response evaluation of buried steel pipelines at active fault crossings is among the top seismic design priorities. This is because the axial and bending strains induced to the pipeline by step-like permanent ground deformation may become fairly large and lead to a rupture, either due to tension or due to buckling. Certainly, a 3D large scale finite element analysis is a powerful method and allows a rigorous solution of the problem with minimizing the number of necessary approximations. Nevertheless, modeling the non-linear behavior of soil-pipeline system, induced by large displacements, and setting numerical parameters for the entire model are indeed cumbersome and the computational effort can be very

time consuming. Hence, there remains still an important place for simple approaches even in these days of highly complex numerical solutions to difficult problems, at least for preliminary design and verifcation purposes [3-4].

A simplifed analytical methodology, which is widely used today for strike-slip and normal faults, is the one originally proposed by Kennedy et al. [5], and consequently adopted by the ASCE guidelines for the seismic design of pipelines [6]. Kennedy et al. [5] extended the ideas of Newmark and Hall [7], and incorporated some improvements in the method for evaluating the maximum axial strain. Recently, Karamitros et al. [8] developed the Kennedy model for the stress analysis of buried steel pipelines based on the assumptions in the Wang-Yeh [9] model. Specifically, like Wang and Yeh, they use a beam-on-elastic foundation model for the straight pipe region. The aim of present work is to examine and compare the mechanical response of continuous (welded) buried steel pipelines crossing active strike-slip seismic faults by three different skims including analytical method, Winkler model and 3D FEM continuum using ABAQUS software [10]. The obtained results will hopefully contribute to the understanding of fault surface rupture effects on the buried pipelines so as to be able to develop the necessary seismic code provisions.

2. Earthquake Faulting Hazard

If the earthquake magnitude is large enough, the offset will propagate all the way to the surface, resulting in a surface rupture or surface expression of the fault offset. Youngs et al. [11] presents a number of relations for the probability of surface rupture as a function of earthquake moment magnitude. As shown in Figure (1), there is less than a 10% chance of surface rupture for an event of magnitude 5, about a 50% chance for events with magnitudes in the 6 to 6.5 range, and more than a 90% chance for a magnitude 7.5 event.

As described in section 1, the past earthquakes have shown how human lives, buildings and infrastructures are endangered by fault surface ruptures. Although surface faulting is not a new problem, there are very few seismic codes in the world containing any type of provisions for reducing the risks. Discussions on this issue are to be based on a quite different scenario from those of ordinary

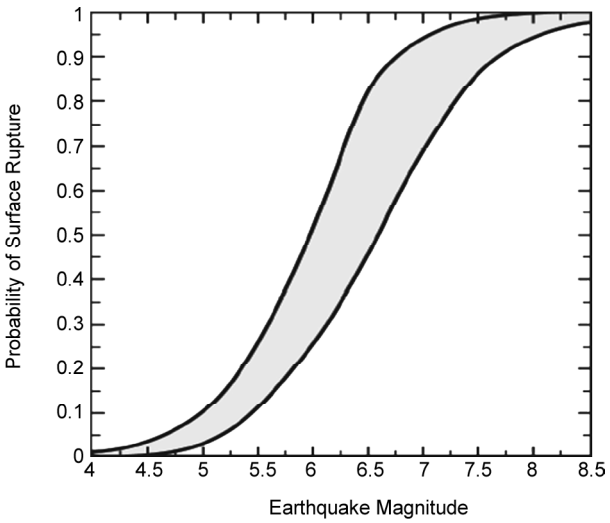

Figure 1. Probability of surface rupture as a function of earthquake magnitude (after Youngs et al. [11]).

design ground motions in which only ground accelerations and/or velocities are crucial factors. The fault-induced displacements and consequent strains in structures should also be taken into consideration. Hence, additional work in this emerging area of earthquake engineering is warranted [12-13].

Principal types of fault movement include strike-slip, normal slip and reverse slip. In a strike-slip fault, the offset is in a horizontal plane, which deforms a continuous pipe primarily in axial tension and bending or axial compression and bending depending on the pipe-fault intersection angle. Various empirical relations between fault displacement and earthquake size have been proposed. The Wells and Coppersmith [14] relations are arguably the most widely recognized in practice. They establish empirical relations between surface rupture length, maximum rupture displacement, and average rupture displacement as a function of the earthquake moment magnitude. Their relation for the average rupture displacement, $D(M)$, in a strike-slip fault as a function of the earthquake moment magnitude, M, is:

$$\log D = -6.32 + 0.90M \tag{1}$$

In general, there are two potential failure modes for continuous buried pipelines crossing a fault. They are: tensile rupture and local buckling (wrinkling) in compression. Hence, this paper focuses on tensile rupture of a pipe due to the bending and tension, and wrinkling of the pipe wall due to the bending and compression. This information will be definitely

essential for the design of pipelines, whose constructions across active faults cannot be avoided in earthquake-prone countries.

3. Simulation of Strike-Slip Fault

A strike-slip fault could place a pipe in either nominal tension or nominal compression depending upon the intersection angle between the fault trace and pipe axis and the relative movement at the fault. For example, the left lateral movement of the fault in Figure (2) results in pipeline elongation and, hence, the nominal tension case. On the other hand, a right lateral fault offset would result in the nominal compression case. The fault movement is defined in a Cartesian coordinate system, where the x-axis is collinear with the un-deformed longitudinal axis of the pipeline, while the *y* axis is perpendicular to *x* in the horizontal plan. Subsequently, the fault movement is analyzed into two components, D_x and D_y, interrelated through the angle β formed by the x-axis and the fault trace, as defined in Eqs. (2) and (3).

$$D_x = D\cos(\beta) \tag{2}$$

$$D_y = D\sin(\beta) \tag{3}$$

There has been more research effort directed at the nominal tension case ($\beta \le 90^0$) than the nominal compression case ($\beta > 90^0$). This is likely an outgrowth of the fact that the nominal tension case is preferred in design since the tensile strain capacity of steel pipe is larger than compressive strain capacity. In addition, because of the buckling behavior, the nominal compression case is more complicated. A non-linear quasi-static solution is desirable for the problem of a pipeline crossing an active fault, which assumes that the fault displacement components are applied at a sufficiently slow rate so as to ensure that the dynamic effects are negligibly small [15]. The velocity of movement on one side of the fault with respect to the opposite side is generally sufficiently low. Hence, the effects of fault rupture on the pipeline can be considered similar to those for statically applied relative movement. Quasi-static conditions were simulated in the analysis by applying the fault offset components to non-zero displacement boundary conditions through a smooth loading function of time (smooth step function) that avoids any sudden load changes, and by keeping a sufficiently long loading duration for the fault offset components.

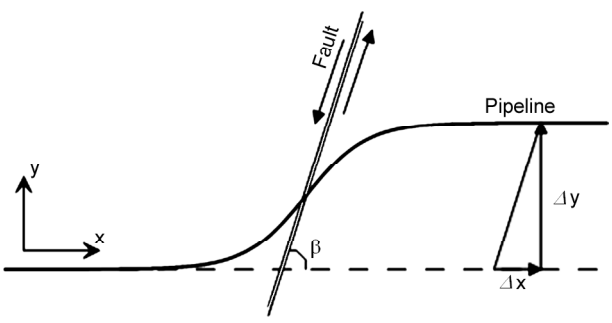

Figure 2. Definition of axes x and y and fault displacements D_x and D_y.

4. Methodology

The currently available techniques of finite element analysis allow taking the fault induced permanent soil deformations and related strains built-up in structures into account in a rigorous manner. However, the non-linear behavior of the pipeline steel, the soil-pipeline interaction and the second order effects, induced by large displacements, make such analyses rather demanding, and provide ground for the use of simplified analytical and semi-analytical methodologies. To validate the results of the simplified methods, their predictions will be compared to the results from a series of 3D non-linear numerical FEM analyses.

4.1. Finite Element Method

The structural response of the steel pipelines under fault movement is examined numerically using advanced computational tools. General-purpose finite element program, ABAQUS, is employed to simulate accurately the mechanical behaviour of the steel pipe, the surrounding soil medium and their interaction, considering the non-linear geometry of the soil and the pipe through a large-strain description of the pipe-line-soil system and the inelastic material behaviour for both the pipe and the soil.

For 3D FEM continuum model, an elongated prismatic model is considered, where the pipeline is embedded in the soil. The corresponding finite element mesh for the soil formation is depicted in Figure (3a) and for the steel pipe in Figure (3b). Four-node reduced-integration shell elements (type S4R) are employed for modeling the pipeline cylinder, whereas eight-node reduced-integration

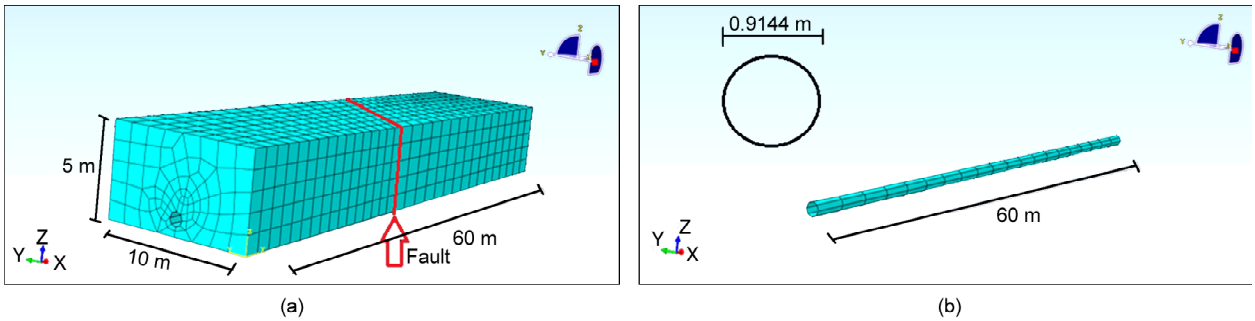

Figure 3. Finite element model of the (a) soil formation with tectonic fault, and (b) steel pipeline.

brick elements (C3D8R) are used to simulate the surrounding soil. The top surface represents the soil surface, and the burial depth is chosen similar to pipeline engineering practice [16]. A 60-diameter length of the pipeline in the x-direction is considered for the purposes of the present analysis in accordance with the several recent numerical studies (e.g. [17-18]). They also reported that prism dimensions in directions *y* and *z* equal to 10 and 5 times the pipe diameter, respectively, are adequate. The numerical model is considered to have various values of angle β between the pipeline axis and the fault plane at the pipeline middle section and divides the soil in two equal parts. The analysis is conducted in two steps; gravity loading is applied first and subsequently fault movement is imposed. The vertical boundary nodes of the first block remain fixed in the horizontal direction (including the end nodes of the steel pipeline), whereas a uniform displacement due to the fault movement is imposed in the external nodes of the second moving block in the horizontal *y* direction including the end nodes of the pipeline.

4.2. Winkler Method

In this section, an attempt is made to develop simple FE model (i.e. Winkler model) using 3D beam elements for the response analysis of buried pipelines subjected to strike-slip fault motion. FEM model was developed using the software ABAQUS. Figure (4) shows the geometry adopted for the proposed finite element model. The pipeline segment was modeled using 2-noded elastic-plastic beam elements (type B31) oriented along the longitudinal axis. Pipe material nonlinearity was considered in the analysis by associating a bi-linear

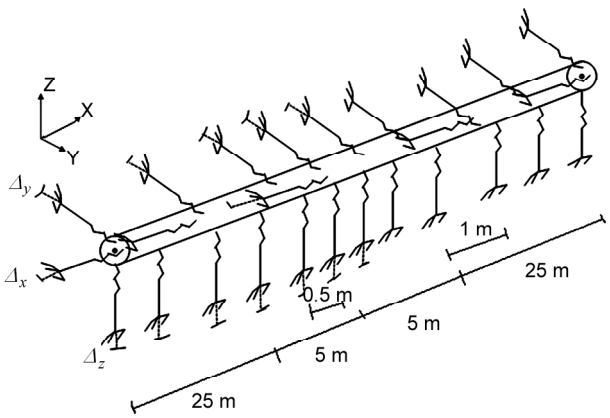

Figure 4. Geometry of proposed Winkler model for buried pipeline.

stress-strain curve to the beam element. The FE formulation for this element is based on Timoshenko's beam theory and takes into account transverse shear deformations.

Movement of the soil mass along the fault plane results in pipeline-soil interaction in all the three pipeline directions. Soil surrounding the pipeline was modeled using non-linear springs that support the pipeline at discrete points, following the methodology detailed in ASCE design guideline [6]. The SPRING2 element was used to model the elasto-plastic springs in the axial, lateral and vertical directions. This element is between two nodes, acting in a fixed direction. The mesh is refined in the critical region within the vicinity of the fault with element lengths of 0.5m specified. The remainder of the pipeline was modeled with 1m long elements in the relatively undisturbed area, Figure (4). Complex 3D strike-slip fault motion was simulated by applying non-zero displacements to the soil-spring ends through suitable constraints between pipe-nodes and corresponding soil-spring ends.

4.3. Analytical Method

Newmark and Hall [7] were the first to formally analyze the fault crossing problem. Kennedy et al. [5] extended the pioneering work of Newmark and Hall by taking into account soil-pipeline interaction in the transverse as well as in the longitudinal directions. They proposed a simplified methodology adopted by the ASCE guidelines [6] for the seismic design of pipelines under strike-slip faults. Subsequent to the above studies, Wang and Yeh [9] introduced some additional modifications. Specifically, they use a beam on an elastic foundation (BEF) model for the straight portion of the pipeline beyond the constant curvature region. Their methodology refers only to strike-slip faults and relies on partitioning of the pipeline into four distinct segments, Figure (5). Furthermore, they subdivide the constant curvature region into elastic strain and inelastic strain regions. Wang and Yeh [9] apparently neglect the influence of pipe axial stress on pipe bending stiffness, and conclude that the pipe fails at the start of the BEF region. This seems somewhat unlikely since one expects tensile rupture to occur at or very near the location of maximum tensile strain that is closer to the fault.

Most recently, Karamitros et al. [8] extended the Kennedy model by incorporating some ideas from the Wang-Yeh model. Specifically, like Wang and Yeh, they use a BEF model for the straight pipe region. As a simplification, they neglect the elongation due to the arc-length effects induced by the lateral component of the fault movement in evaluations of the total pipe elongation. To account for situations with comparatively small offsets and low axial strain, they calculate the bending strain as follows:

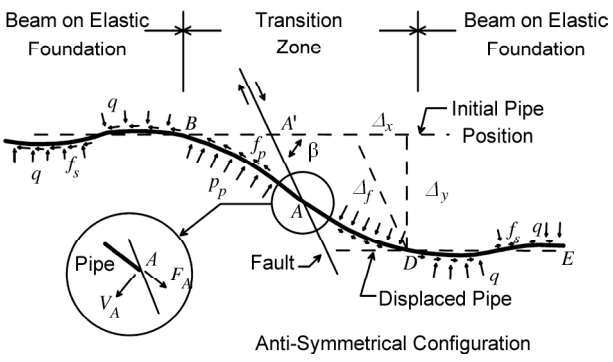

Figure 5. Pipeline analysis model proposed by Wang and Yeh [9].

$$\frac{1}{\varepsilon_b}=\frac{1}{\varepsilon_b^I}+\frac{1}{\varepsilon_b^{II}} \tag{4}$$

where ε_b^I is the strain due to the bending moment and ε_b^{II} is the bending strain due to curvature of the pipe.

$$\varepsilon_b^I=\frac{M_{\max}D}{2EI} \tag{5}$$

$$\varepsilon_b^{II}=\frac{D}{2R_C} \tag{6}$$

where R_C is the radius of curvature of the curved portion in the pipe. As such, the Karamitros et al. [8] relation is applicable for both small offsets (offset over diameter less than 1.0) and larger offsets envisioned by the Kennedy et al. procedure. Note that, their proposed method does not account for the effects of local buckling and section deformation. Therefore, its application should not be extended beyond the strain limits explicitly defined by design codes in order to mitigate such phenomena.

5. Model Description

Numerical and analytical results are obtained for buried pipelines that crosses strike-slip faults at different angles. Seismic fault plane is assumed to be located at the middle cross-section of the pipeline. In all cases considered in the present paper, the outer pipe diameter of pipe *D* is assumed equal to 914.4 mm (36 in.), where the pipe wall thickness, *t*, ranges from 6 mm to 20 mm, so that a range of D/t values between 46 and 152 is covered. This range of D/t values is typical for onshore applications (oil, gas or water pipelines). The steel pipeline was of the API5L-X65 type, with a bi-linear elasto-plastic stress-strain curve, Figure (6), and the properties listed in Table (1). The pipeline is assumed to follow the most widely used Ramberg-Osgood model [20], as given in Eq. (7) and with the properties listed in Table (2).

Table 1. AP15L-X 65 steel properties [19].

Yield Stress (σ_1)	490 MPa
Failure Stress (σ_2)	531 GPa
Failure Strain (ε_2)	4.0%
Elastic Young's Modulus (E_1)	210 GPa
Yield Strain ($\varepsilon_1=\sigma_1/E_1$)	0.233%
Plastic Young's Modulus $E_2=(\sigma_2-\sigma_1)/(\varepsilon_2-\varepsilon_1)$	1.088 GPa

$$\varepsilon = \frac{\sigma}{E_1}\left[1+\left(\frac{n}{r+1}\right)\left(\frac{|\sigma|}{\sigma_y}\right)^r\right] \quad (7)$$

For the 3D finite element model, the surrounding soil has dimensions 60m×10m×5m in directions *x*, *y* and *z*, respectively. The mechanical behavior of soil material is described through an elastic-perfectly plastic Mohr-Coulomb constitutive model, characterized by the soil friction angle φ, the elastic modulus *E*, and Poisson's ratio *v*. The dilation angle ψ is assumed to be zero throughout this study. Physical parameters of soil are shown in Table (3).

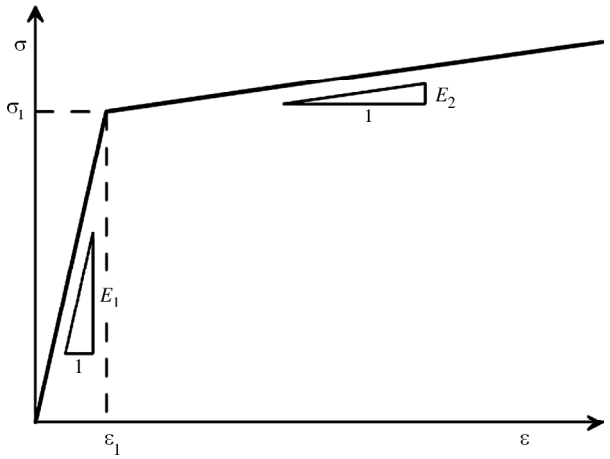

Figure 6. Assumed bi-linear stress-strain relationship for the pipeline steel.

Table 2. Ramberg-Osgood stress-strain parameters for AP 15L-X 65 steel type .

Yield Stress (σ_y)	490 MPa
Initial Young's Modulus (E_1)	210 GPa
n	38.32
r	31.5

Table 3. Physical parameters of the soil.

Type	Density ρ (Kg/m^3)	Elastic Young's Modulus (MPa)	Friction Angle Φ (^{0})	Poisson's Ratio υ
Sand I	1850	8	30	0.3
Sand II	2100	50	40	0.3

A contact algorithm is considered to simulate rigorously the soil-pipeline interaction that accounts for large strains and displacements. The algorithm takes into account the interface friction through the definition of an appropriate friction coefficient between the outer surface of the steel pipe and the surrounding soil. The analysis proceeds using a displacement-controlled scheme, which increases gradually the fault displacement *D*. At each increment of the non-linear analysis, stresses and strains at the pipeline wall are recorded. Furthermore, due to the fine mesh employed at the critical pipeline portions, the local buckling (wrinkling) formation and the post-buckling deformation at the compression side of the pipeline wall are simulated.

For Winkler model, the properties of soil-springs were calculated according to the ALA-ASCE guidelines [21]. Table (4) shows the soil-spring properties considered in this study. To simulate soil-pipeline interaction effects, each node of the pipe is connected to axial, transverse horizontal and vertical soil-springs, modeled as elastic-perfectly plastic elements. The fault movement is applied statically at the sliding part of the fault, as a permanent displacement of the free end of the corresponding soil-springs.

6. Results: Validation and Comparison

Quasi-static analyses were carried out by applying fault offset components to soil-spring ends in the Winkler models and to moving blocks in the continuum FE models through a smooth loading function of time. In this study, ABAQUS/Explicit solver was chosen for the non-linear analysis due to its capabilities of analyzing post-buckling behavior more efficiently and to avoid the convergence problems typically encountered by implicit solvers in the post-buckling domain. Geometric nonlinearity associated with the large deformations was also incorporated in the analysis.

Table 4. Soil-spring properties considered in the Winkler model .

Type of Spring	Yield Force (kN/m)	Yield Displacement (mm)
Axial (Friction) Springs	40.5	3.0
Transverse Horizontal Springs	318.6	11.4
Vertical Springs (Upward Movement)	52.0	2.2
Vertical Springs (Downward Movement)	1360	100.0

The factors influencing response of buried pipeline at strike-slip fault crossing include the fault offset (*D*), pipeline crossing angle (β), backfill soil type, burial depth (*H*), pipe diameter (*D*), thickness (*t*) and pipe material. However, the designer has the choice to vary these factors so as to improve the pipeline's performance and optimize the design. In?uence of these design parameters on the response of buried steel pipe due to strike-slip fault motion was studied using the previously described methodologies in section 4. The analyses were performed with a view to enable the selection of design parameters that would enhance the pipeline's capacity to accommodate the strike-slip fault offset. Figure (7) plots the axial strain distribution in the buried pipeline after a seismic fault movement using the Winkler method and the FEM model.

6.1. Effect of Crossing Angle

A moderately thick-walled X65 pipeline is considered first, with length, burial depth, diameter and thickness equal to L = 60.0 m, H = 1.3 m, D = 914.4 mm and t = 12 mm, respectively, so that D/t =76. Figure (8) plots the maximum strains of steel pipe embedded in medium density sand with friction angle = 35° and unit weight = 18 kN/m^3 versus the fault offset. The results of the FEM analyses are presented in comparison with the

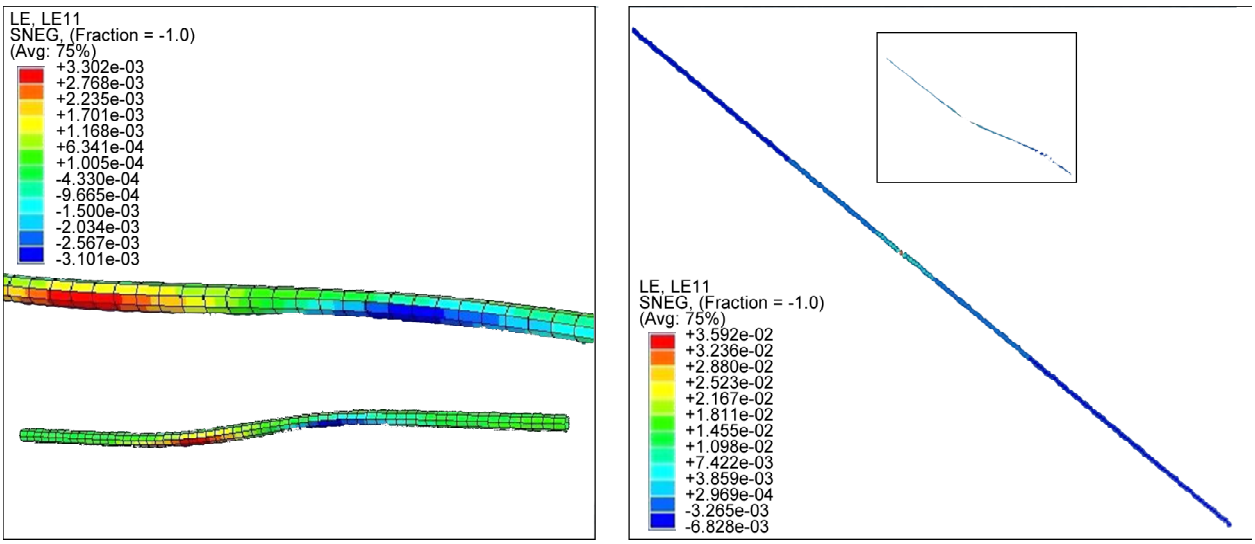

Figure 7. Axial strain distribution in the deformed pipe: a) 3D FEM model, and b) Winkler model.

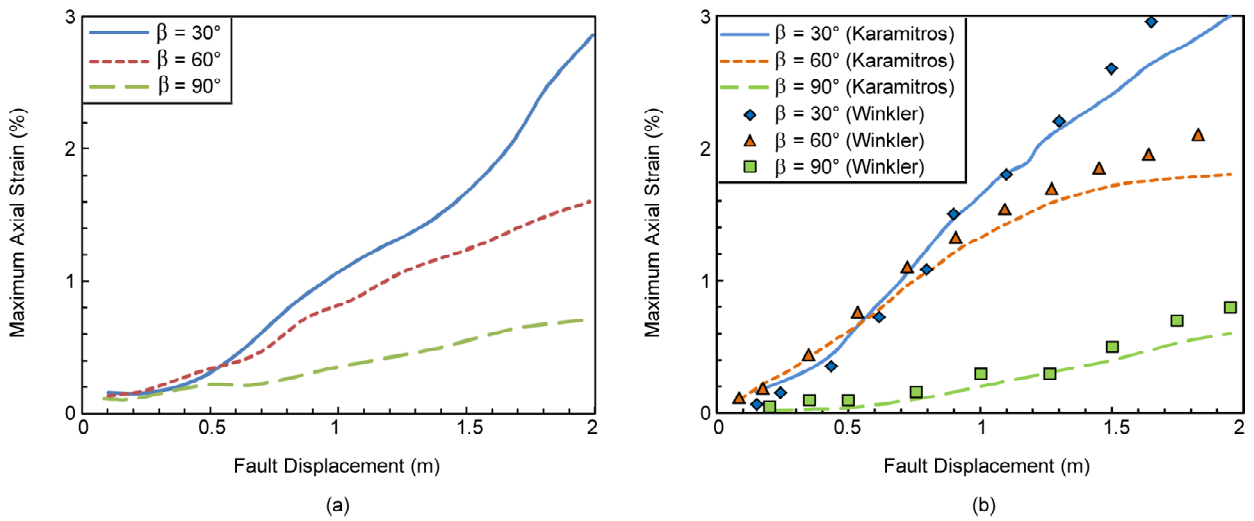

Figure 8. Effect of crossing angle on the peak pipe strain for medium dense sand: a) FEM model, and b) Winkler and analytical method.

Winkler prediction, as well as the analytical methodology of Karamitros et al. [8]. Three different fault cases are examined, with intersection angles of β = 30°, 60° and 90°. In each case, the analysis proceeded incrementally to a final fault displacement of $D \# 2D$, possible scenario for an earthquake with the expected average moment magnitude of $M = 7.4$ based on the empirical relationship in Eq. (1).

As one might expect, the peak strains from the FEM are larger for an intersection angle β = 30° from those for 60°, particularly for offsets larger than pipe's diameter. In addition, longitudinal strains become rather small and insignificant when the fault is getting normal to the pipeline direction. Therefore, results of this study suggest that the pipeline strain can be significantly reduced at strike-fault crossing by choosing a near-perpendicular orientation of the pipeline with the fault line in plan. On the other hand, the Karamitros model compares favorably to the FEM results for all offsets considered. However, the Winkler model provides reasonable strain estimates for smaller offsets. As the offsets increases, the Winkler peak strain becomes larger. Note that the recommended values for pipe-soil interaction forces in the ALA-ASCE guidelines [21] are nominally an upper bound for the measured data. In general, the forces on the pipeline and the pipe strains are larger using upper bound soil-springs and; therefore, the Winkler method is conservative. Hence, in terms of investigated simplified approaches, the Karamitros method seems more reasonable for the evaluation of design capacity. The Winkler approach would be recommended for determination of the state of pipe strain at smaller fault offsets, on the order of the pipe diameter itself.

6.2. Effect of Burial Depth

The same pipeline section as above was analyzed for three burial depths. Figure (9a) shows the plots of maximum axial strains against the applied D from the 3D FEM, when the backfill is loose. Peak strains were observed to increase as the burial depth increased from 1.30 to 3 m. Similar effect for the burial depth was observed when the pipeline embedded in dense granular was analyzed as shown in Figure (9b). Results of the parametric study show that the increase in burial depth increased the values of limiting uplift soil force and limiting pipe-soil friction force acting on unit length of the pipeline, and consequently led to higher maximum axial strain for a constant magnitude of D. Thus, a burial depth as shallow as possible is preferable in the fault crossing zone. However, the live loads and environmental factors may also have an influence on the minimum soil cover.

6.3. Effect of Backfill Type

Figure (10) shows the effect of backfill type on maximum axial strain in the pipeline (with burial depth of $H = 1.75$ m) at various strike-slip fault offset magnitudes. The same pipeline segment as adopted in Section 6.1, was studied for three granular backfills: loose (φ = 30°), medium dense (φ = 35°) and dense (φ = 40°). Fault motion

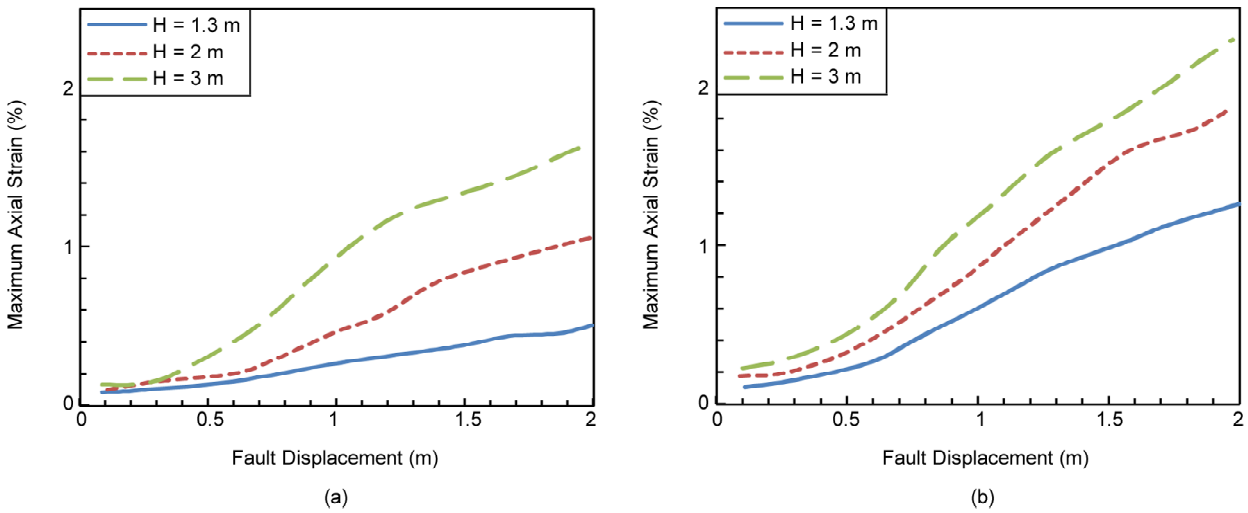

Figure 9. Effect of burial depth on the maximum axial strain: a) Sand I, and b) Sand II (β = 90°).

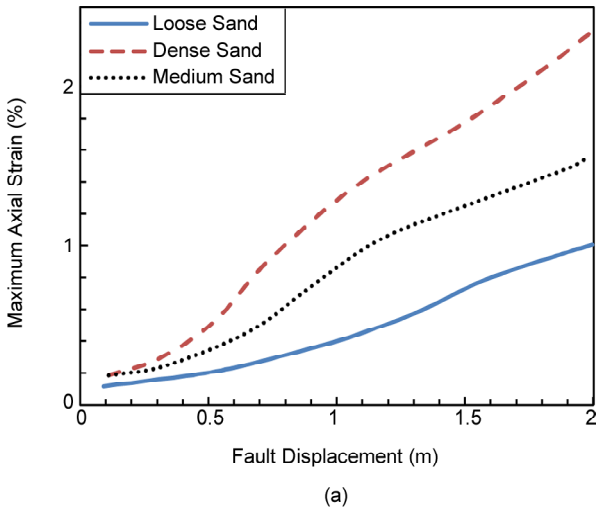

Figure 10. Effect of backfill type on the maximum total strain in the pipeline (β = 90°, H = 1.75 m).

parameter β was chosen to be 90°, and the pipeline was subjected to the maximum fault offset of 200 cm in increments of 20 cm. For a constant magnitude of *D*, the maximum strain value increased as the compactness of backfill increased. Note that, the results obtained from Figure (10) suggest that the pipeline could be expected to perform well by a fair amount by placing a loose backfill in the fault crossing region and by avoiding its unnecessary over-compaction.

6.4. Pipeline Performance

The behavior of buried X65 steel pipelines with D/t = 76 and H = 1.75 m in loose sand under fault-induced deformation is analyzed using the FE numerical tool. Figure (11a) and (11b) plots the distribution of axial normal strain at the tension and compression sides of the pipeline respectively, for different values of fault displacement *D*. It should be noted that determining the value of fault displacement at which onset of localized buckling occurs (D_{cr}), referred to as critical fault displacement, can be defined in several ways. Considering the convention of local buckling onset given in Vazouras et al. [17], local buckling occurs at a fault displacement of about D_{cr} = 0.45 m for the present case, Figure (11b). Moreover, the 3% tensile strain is reached at D_{cr} = 1.95 m, whereas the 5% tensile strain performance criterion is not reached within the maximum fault displacement (4 m) considered in the analysis; in fact, the tensile strain reaches a value of about 3.8% in the course of this analysis.

6.5. Effect of the Diameter to Thickness Ratio

The effects of the diameter to thickness ratio is examined for 0.914 m-diameter steel pipelines with thickness ranging between 6 mm and 20 mm, corresponding to D/t values between 46 and 152. The numerical results for the mechanical behavior of X65 pipelines embedded in sand I and sand II are summarized in Figure (12). Herein, the onset of local buckling is adopted at the stage where the compressive strain of the pipe reaches the allowable wrinkling strain given in the ALA-ASCE [21] as follows:

$$\varepsilon_c = 0.175\frac{t}{R} \tag{8}$$

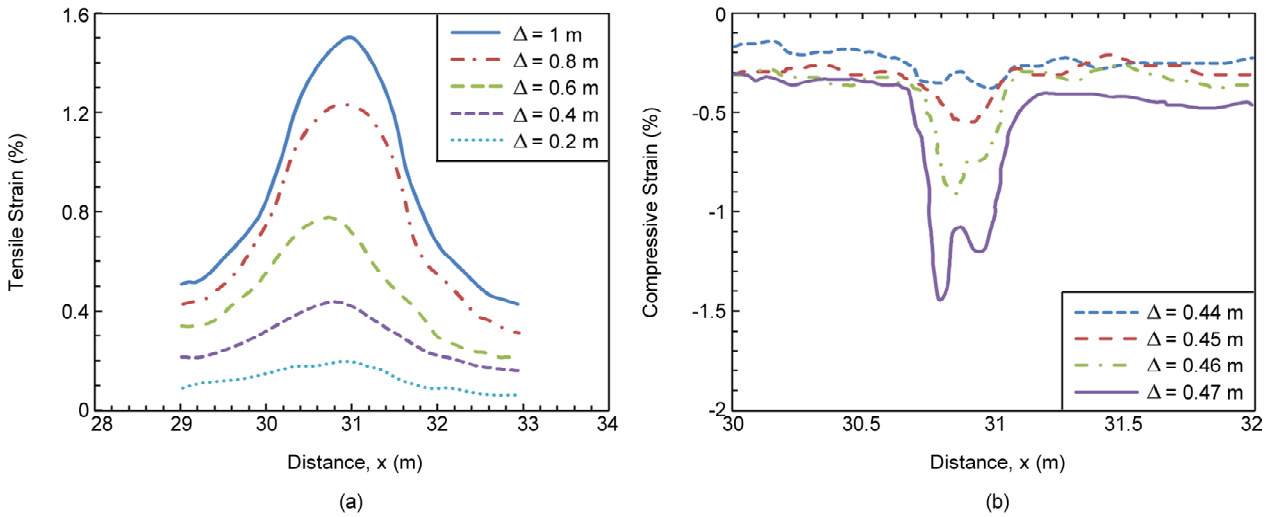

Figure 11. Axial normal strain along the pipeline: a) side under tension, and b) side under compression (Sand I, β = 90°, H = 1.75 m).

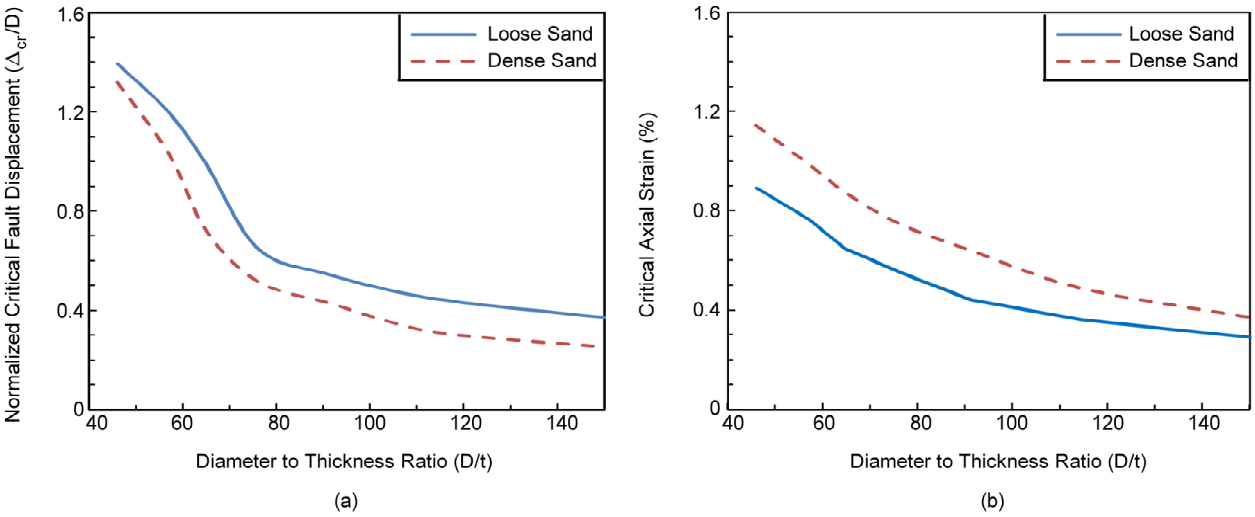

Figure 12. a) Critical fault movement versus the diameter to thickness ratio D/t, and b) critical axial strain versus the ratio D/t ($\beta = 90^{\circ}$, H = 1.75 m).

In particular, Figure (12a) plots the fault critical displacement, D_{cr}, normalized by the pipe diameter D, in terms of the diameter to thickness ratio, D/t. The results show a substantial decrease of D_{cr} with increasing value of the D/t ratio, which means that thin-walled pipelines are more prone to buckling and fail at relatively small values of fault displacement. Furthermore, dense soil conditions (sand II) result in lower deformation capacity of the pipeline. In Figure (12b) the corresponding critical compressive strain at the onset of local buckling, D_{cr}, is plotted against the value of the diameter to thickness ratio, D/t. The results indicate that the thinner pipes buckle at smaller critical strain, which is in accordance with the experimental data reported by Kyriakides and Ju [22].

6.6. Effect of Pipe Surface Characteristics

Further analyses were performed on the same pipeline section to evaluate the influence of soil-pipe interface friction on pipeline's performance. Figure 13 shows the response of the pipeline to given strike-slip fault motion for two different surface characteristics. Steel pipeline with a smooth and hard surface coating was assumed to have the coefficient of friction f = 0.5 and pipeline without any special coating was assumed to have f = 0.8 [6]. Considerable reduction in the value of the maximum strain can be seen due to the use of surface coating in the fault crossing zone. At D = 2 m, the pipeline peak strain can be seen to reduce from 1.05% for f = 0.8 to 0.52% for f = 0.5 in Figure (13a), and from 1.95% for f = 0.8 to 0.55% for f = 0.5 in Figure (13b);

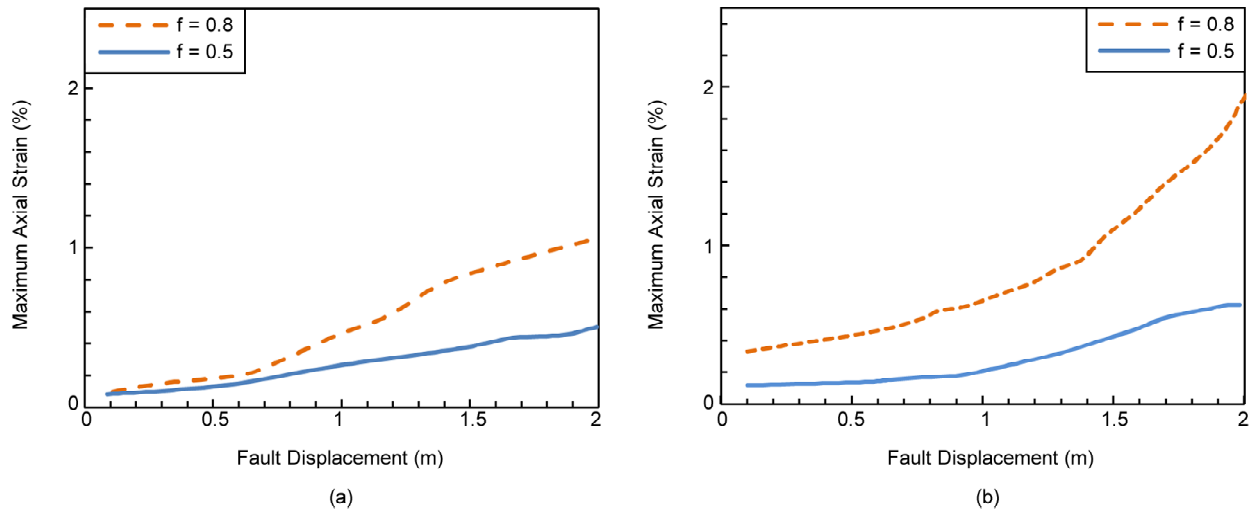

Figure 13. a) Effect of pipe surface characteristics on the maximum total strain: a) Sand I, and b) Sand II ($\beta = 90^{\circ}$, H = 1.75 m).

where the granular backfill to be loose ($\varphi = 30^o$) and dense ($\varphi = 40^o$), respectively. Smooth surface coating reduces the value of coefficient of friction between pipe and the soil, and leads to a reduction in the value of limiting soil frictional force acting over unit length of the pipe. Consequently, for a constant magnitude of *D*, the value of maximum axial force developed in the pipeline near the fault crossing would be reduced and this force will be dissipated over larger length of the pipeline.

7. Conclusion

A strike-slip fault could place a pipe in either nominal tension or nominal compression depending upon the intersection angle between the fault trace and pipe axis and the relative movement at the fault. Three methods of assessment were discussed in this paper to show how the choice of an analysis approach affects the seismic response of a buried pipeline subjected to faulting. In conclusion, it was found that the use of the Winkler and analytical methods for seismic fault line displacement analysis may not be sufficient for proper pipeline design and leads to over-simplistic conclusions. The principal reason for the conservatism is related to the poor modeling of realistic surrounding soil behavior for large deformation events. During the early design phases, there is a great advantage in using the Winkler or analytical methods to get a better understanding of the potential impact of the earthquake faulting on the pipeline. Thus the pipeline can be rerouted based on the outcome of the initial analysis. However, for an existing pipeline lying across a seismic fault with substantial offset, it is worthwhile undertaking an assessment of the pipeline structural integrity using the continuum FEM. The influence of design parameters including crossing angle, backfill properties, burial depth and pipe surface property on maximum strain and buckling of buried steel pipelines were then analyzed for strike-slip fault motions. The obtained results could be summarized as follows:

- Out of all the investigated design parameters, the pipeline crossing angle was found to be the most influencing factor on the response of buried pipelines in terms of maximum strain and its buckling. The capacity of buried pipeline to accommodate the strike-slip fault offset could be increased substantially by adopting a near-normal orientation in plan with respect to the fault line.
- The capacity of the pipeline to safely accommodate the strike-slip fault offset can be further increased by choosing a loose granular backfill, adopting a shallower burial depth, using a smooth and hard surface coating or by increasing pipe wall thickness.

Therefore, the information obtained in this study can provide guidance for developing improved earthquake-resistant design of pipelines crossing active strike-slip faults. Currently, a research is under way to assess buried pipeline performance subjected to reverse fault movements.

Acknowledgements

This work was supported in part by the University of Kashan. The first author would like to acknowledge this research sponsorship. The article benefited from constructive comments by two anonymous reviewers.

References

1. EERI (1999) *The Izmit (Kocaeli) Turkey Earthquake of August 17, 1999*. EERI Special Earthquake Report.
2. Uzarski, J. and Arnold, C. (2001) *Chi-Chi, Taiwan, Earthquake of September 21, 1999, Reconnaissance Report*. Earthquake Spectra, Professional J EERI, 17 (Suppl. A).
3. Tahghighi, H. (2014) *On the Structural Seismic Evaluation of Pipelines Against Earthquake Hazards*. Report on Research Project, Grant--in-Aid for Scientific Research, University of Kashan.
4. Joshi, S., Prashant, A., Deb, A., and Jain, S.K. (2011) Analysis of buried pipelines subjected to reverse fault motion. *Soil Dynamics and Earthquake Engineering*, 31, 930-940.
5. Kennedy, R.P., Chow, A.W., and Williamson, R.A. (1977) Fault movement effects on buried oil pipeline. *Journal of the Transportation Engineering Division*, ASCE, **103**, 617-633.
6. ASCE Technical Council on Lifeline Earthquake Engineering (1984) *Differential Ground Movement Effects on Buried Pipelines*. Guidelines Seismic Des. Oil Gas Pipeline Syst., 150-228.

7. Newmark, N.M. and Hall, W.J. (1975) Pipeline design to resist large fault displacement. *Proceedings of the 1975 U.S. National Conference on Earthquake Engineering*, Ann Arbor, Michigan, 416-425.

8. Karamitros, D.K., Bouckovalas, G.D., and Kouretzis, GP. (2007) Stress analysis of buried steel pipelines at strike-slip fault crossings. *Soil Dynamics and Earthquake Engineering*, **27**, 200-211.

9. Wang, L.R.L. and Yeh, Y. (1985) A refined seismic analysis and design of buried pipeline for fault movement. *Journal of Earthquake Engineering and Structural Dynamics*, **13**, 75-96.

10. ABAQUS (2012) General Finite Element Analysis Program, ABAQUS Manual, Version 6.11, HKS, Inc.

11. Youngs, R., Arabasz, W., Anderson, R., Ramelli, A., Ake, J., Slemmons, D., McCalpin, J., Dorser, D., Fridrich, C., Swan, F., Rodgers, A., Yount, J., Anderson, L., Smith, K., Bruhr, R., Knuepter, P., Smith, R., DePolo, C., O'Leary, D., Coppersmith, K., Pezzopane, S., Schwartz, D., Whitney, J., Olig, S., and Toro, G. (2003) A methodology for probabilistic fault displacement hazard analysis. *Earthquake Spectra*, **19**(1), 191-219.

12. Tahghighi, H., Konagai, K., and Johansson, J. (2008) *Hybrid Stochastic Simulation of Near-Fault Strong Motion Records From the 1999 Chi-Chi, Taiwan Earthquake*. Report on JSPS Research Project for Rational Design of Lifelines Near Seismic Faults, Grant-in-Aid for Scientific Research. The University of Tokyo.

13. Tahghighi, H. (2011) Earthquake fault-induced surface rupture - A hybrid strong ground motion simulation technique and discussion for structural design. *Earthquake Engineering and Structural Dynamics*, **40**, 1591-1608.

14. Wells, D.L. and Coppersmith, K.J. (1994) New empirical relationships among magnitude, rupture length, rupture width, rupture area, and surface displacement. *Bulletin of the Seismological Society of America*, **84**(4), 974-1002.

15. Davoodi Moghaddam, M. (2014) *Seismic Behavior of Buried Pipelines due to Surface Faulting*. M.Sc. Thesis, University of Kashan, Iran (in Persian).

16. Mohitpour, M., Golshan, H., and Murray, A. (2007) *Pipeline Design and Construction: A Practical Approach*. 3rd ed., New York, NY, ASME Press.

17. Vazouras, P., Karamanos, S.A., and Dakoulas, P. (2012) Mechanical behavior of buried steel pipes crossing active strike-slip faults. *Soil Dynamics and Earthquake Engineering*, **41**, 164-180.

18. Vazouras, P., Dakoulas, P., and Karamanos, S.A. (2015) Pipe-soil interaction and pipeline performance under strike-slip fault movements. *Soil Dynamics and Earthquake Engineering*, **72**, 48 -65.

19. American Petroleum Institute, API (2007) Specification for Line Pipe, 44th ed., ANSI/API, Spec 5L.

20. Ramberg, W. and Osgood, W. (1943) Description of Stress-Strain Curves by Three Parameters, Technical Note, No. 902, National Advisory Committee for Aeronautics, 28p.

21. American Lifelines Alliance (ALA)-ASCE (2001) Guidelines for the Design of Buried Steel Pipe, (with addenda through February 2005).

22. Kyriakides, S. and Ju, G.T. (1992) Bifurcation and localization instabilities in cylindrical shells under bending I: experiments. *International Journal of Solids and Structures*, **29**, 1117-1142.